First-principle investigation of Ti wetting layer influence on metal-graphene contact

Xiang Ji Yan Wang* Zhiping Yu
Institute of Microelectronics, Tsinghua University, Beijing, China
Email: wangy46@tsinghua.edu.cn

Introduction

Metal (M) /grapheme (Gr) contact has attracted much attention since the contact resistance (R_c) between Gr and metal electrode is crucially important for achieving high performance of grapheme-based devices [[1]-[15]]. Published experimental works on metal/graphene contacts generally adopted Gr/Ti/Metal structure to enhance the interfacial adhesion [[1]-[8]]. However, how the presence of Ti wetting layer can influence the global response of Gr-based device remains unclear. To present a clear physical understanding and optimizing transport between metal electrodes and graphene with Ti wetting layer, the binding energy, band structure, interface potential profile and contact resistance of the Gr/Ti/Metal (Al, Cu, Au, Pt, Pd) systems were studied for the first time by first-principle and NEGF methods in this paper. The results provide insights into contact resistance optimization and the ultimate scalability of graphene-based devices.

Details of Calculation

We employ the SIESTA package [[16]] with the projected augmented wave (PAW) [[17]] pseudopotentials within local density approximation (LDA) to investigate the electronic structure of different contacts, as such exchange-correlation function well describes the geometry structures of graphene-metal systems [[18]] and the TranSIESTA code[[16]], which is based on the real-space, non-equilibrium green function (NEGF) formalism and the density functional theory (DFT) to perform the ballistic quantum transport calculations. In these calculations, structural optimizations were first carried out until atomic forces converged to 0.04 eV/Å. Self-consistent calculations are performed with a mixing rate of 0.1, and the mesh cutoff is chosen as 100 Ry. The simulation system, as shown in Fig.1, is built to replicate the interface between a source/channel region of a graphene device (metal/graphene contact lead and the pure graphene channel). An additional number of metal atoms between the contact lead and the freestanding section are added so that the self-consistent electrostatic potential across the junction develops smoothly [[12]]. The supercells for most stable configuration [[13]-[15]] of metal/graphene contact lead are constructed by using fixed rectangular graphene lattice with w = 4.92 Å and l = 8.52 Å, then adjusting metal's lattice size onto the fixed graphene's lattice, all metals' lattice mismatches are smaller than 5%. In all supercells of the metal–graphene interface models studied here, at least 18 Å vacuum regions are added in the direction perpendicular to the 2D structure. Moreover, we use three layers of metal here, which leads to almost the same results from a structure containing six layers of metal.

The contact resistance is estimated by Eq.1 [[19]],

$$R_c = \left(dJ/dV_{bias} \right)^{-1} \Big|_{V_{bias}=0} \quad (1)$$

Results and Discussions

The binding energies of Gr/Ti/M systems with different Ti thickness are listed in Table I, where the results of Gr/M systems without wetting layer are in consistent with published data [[15]]. All the systems containing just one layer of Ti as wetting layer got a great enhancement in binding energy, which demonstrate the physical essentials of Ti as wetting layer—enhancing the adhesion ability. Moreover, the average distance of metal to graphene layer is also improved, take Al for example, the optimized distance is 3.23 Å for Gr/Al and 2.04 Å for Gr/Ti/Al, respectively. These means that the Ti wetting layer makes the relatively inert metal coupled with the graphene. Fig. 2 specifies the band structure of Gr/Al, Gr/Ti/Al and Gr/Pd systems, while the Gr/Al system could preserve the conical electronic structure of graphene, the Ti wetting layer would disturb its π-orbital components, as the situation of Pd contacted graphene, which is known as chemical contact; Fig. 3 plots the corresponding interface profiles of Gr/Al and Gr/Ti/Al systems, while a clear potential barrier lies between the graphene and metal surfaces in Gr/Al system (potential energy above the Fermi energy between Gr and Al surfaces), it vanishes at metal-graphene interface in Gr/Ti/Al system (no barrier between Gr and Ti surfaces). These two effects, i.e. disturbing graphene π-band and eliminating barrier at graphene-metal interface, are both features of chemical contact [[13],[15]]. In other words, just one single layer of Ti could turn physical contact into chemical contact, which reveals why Ti could be a powerful adhesive metal for graphene.

Furthermore, since the chemical bonding would change the Fermi velocity of graphene und

978-1-4673-5736-4/13/$31.00 ©2013 IEEE

Table I Binding energy (in eV/C atom) of Gr/Ti/M systems with different Ti thickness

Ti thickness \ M	Al	Cu	Au	Pt	Pd	Ti
0	-0.0305	-0.0344	-0.0358	-0.0444	-0.0877	-0.4141
1	-0.5624	-0.5281	-0.4860	-0.4988	-0.5085	⋯
3	-0.4425	-0.4413	-0.4365	-0.4402	-0.4389	⋯

Table II Contact resistance (in Ω•μm) of Gr/Ti/M systems with different Ti thickness

Ti thickness \ M	Al	Cu	Au	Pt	Pd	Ti
0	701	628	2285	765	403	612
1	258	453	332	301	242	521
3	212	237	252	285	279	333

-er the contact, the experiment results could be largely influenced by the wetting layer. Thereby, the contact resistances of Gr/Ti/M systems with different Ti thickness are calculated here to estimate its impact, as listed in Table II. The Ti metal results are also showed here as a reference, where the Ti metal with zero Ti wetting layer means totally 3 layers of Ti metal. From the Ti results, we could see that the contact resistance would generally decrease with increasing metal layers due to the increased DOS around Fermi level, as shown in Fig. 4. As for the wetting layer effect, the R_c of all physical contact metals decreases significantly with the appearance of Ti wetting layer, which should attribute to the vanish of tunneling barrier at the contact interface. The R_c of Gr/Ti/M systems with 1 layer of Ti shows clear metal-to-metal variation while the Gr/Ti/Pd has the smallest R_c, which is in agreement with the experiment results [[8],[9]]. The results of 3 layers wetting layer become much closer to each other compared with 0 and 1 layer Ti results, since we used only three layers of contact metal (Al, Cu, Au, Pt, Pd) in our model, 3 layers of wetting layer seems to have dominating influence on them. Fig. 5 plots the transmission function of Gr/Ti/Cu systems, as the thickness of Ti wetting layer grow from 0 to 3, the Fermi velocity of graphene under the contact becomes smaller, which unveil another aspect of Ti wetting layer effect on transportation. Such deterioration of Fermi velocity would slow down the electron transport between graphene under the metal and graphene channel, giving rise to the contact resistance.

Specially for Pd, the decrease of R_c from 0 to 1 wetting layer may due to the increased DOS, however, because Ti is more destructive to graphene's electronic structure and have larger R_c than Pd [[9]], the R_c of Gr/Ti/Pd become larger as the wetting layer thickness increase from 1 to 3.

Conclusions

The influence of Ti wetting layer on metal-graphene contact were theoretically studied by first-principle and NEGF methods. From the calculation results we conclude that: 1) The Ti could provide excellent adhesive ability for graphene-metal systems by turning physical contact into strong chemical contact. 2) However, it also brings inevitable impact on the contact resistance. For physical contact metals, it endows great improvement by diminishing the potential barrier at metal-graphene interface, however, it would also cause deterioration of graphene's Fermi velocity. Since thicker wetting layer doesn't enhance the binding energy, we suggest that for physical contact metals, the Ti wetting layer should be as thin as possible; For chemical contact metals, which shows more intriguing results, the thickness of both wetting layer and contact metal need to be optimized to get the best R_c.

References

[1] Lee E J H, Balasubramanian K, Weitz R T, *et al.*, Nature nanotechnology, 3(8): 486-490, 2008.

[2] Huard B, Stander N, Sulpizio J A, *et al.*, Physical Review B, 78(12): 121402, 2008.

[3] Farmer D B, Golizadeh-Mojarad R, Perebeinos V, *et al.*, Nano Letters, 9(1): 388-392, 2008.

[4] Nagashio K, Nishimura T, Kita K, *et al.*, Electron Devices Meeting (IEDM), IEEE International. IEEE, 2009: 1-4., 2009

[5] Robinson J A, LaBella M, Zhu M, *et al.*, Applied Physics Letters, 98(5): 053103-053103-3. , 2011

[6] Franklin A D, Han S J, Bol A A, *et al.*, Electron Device Letters, IEEE, 32(8): 1035-1037, 2011.

[7] Knoch J, Chen Z, Appenzeller J.,Nanotechnology, IEEE Transactions on, 11(3): 513-519, 2012.

[8] Franklin A D, Han S J, Bol A A, *et al.*, Electron Device Letters, IEEE, 33(1): 17-19, 2012.

[9] Xia F, Perebeinos V, Lin Y, *et al.*,Nature nanotechnology, 6(3): 179-184, 2011.

[10] Gong C, Hinojos D, Wang W, *et al*., ACS nano, 6(6): 5381-5387, 2012.
[11] Khomyakov P A, Starikov A A, Brocks G, *et al.* , Physical Review B, 82(11): 115437, 2010.
[12] Barraza-Lopez S, Vanević M, Kindermann M, *et al.* , Physical review letters, 104(7): 76807, 2010.
[13] Giovannetti G, Khomyakov P A, Brocks G, *et al.*, Physical review letters, 101(2): 26803, 2008.
[14] Maassen J, Ji W, Guo H.,arXiv preprint arXiv:1009.1066, 2010.
[15] Gong C, Lee G, Shan B, *et al.*, Journal of Applied Physics, 108(12): 123711-123711-8, 2010.
[16] J. M. Soler, E. Artacho, J. D. Gale, A. García, J. Junquera, P.Ordejón & D.S. Portal, J. Phys.: Condens. Matter 14, 2745, 2002.
[17] P. E. Blöchl, Phys. Rev. B **50**, 17953,1994.
[18] Q. J. Wang and J. G. Che, Phys. Rev. Letter **103**, 066802, 2009
[19] Sze S M. Physics of Semiconductor Devices. 2nd Edition. New York; John Wiley and Sons, 1981. *Chap.5*.
[20] S. Datta, Electronic Transport in Mesoscopic Systems; Cambridge University Press, Cambridge, England, 1995.

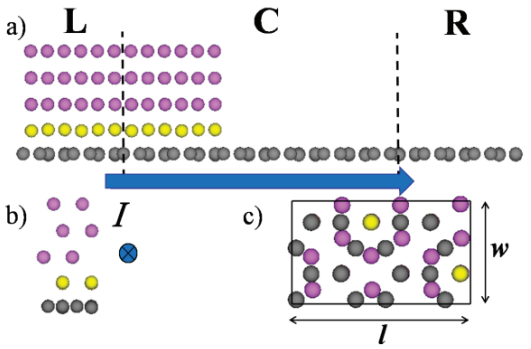

Fig. 1. (a) Two-probe Gr/Ti/Al system used for our NEGF calculation, where left (L) and right (R) leads are semi-infinite and the length of scatter region (C) is 2.556 nm. The grey, yellow and purple balls stand for C, Ti and Al atoms, respectively. (b) Side-view and (c) Bottom-view of the left lead, the black frame is the periodical boundary, where w = 4.92 Å, l = 8.52 Å. The most stable configuration of graphene-metal system corresponds to one sublattice of C atoms situated directly under the first layer of metal atoms.

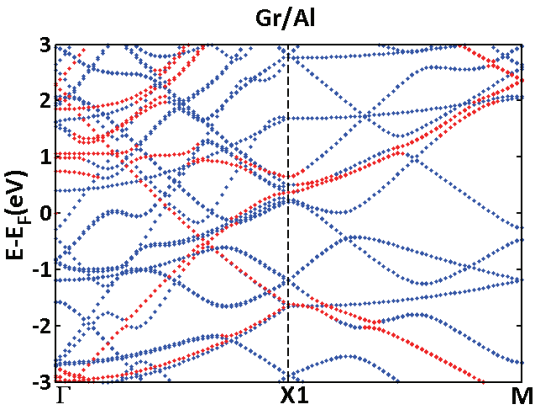

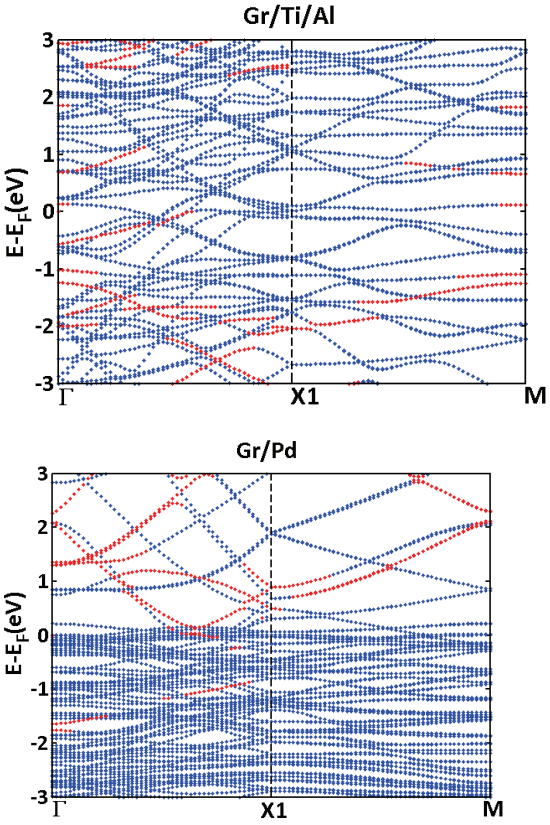

Fig. 2 Band structure of Gr/Al and Gr/Ti/Al systems, the red dots represent the p_z orbital components of graphene. The result of Gr/Al meets well with Ref. [13],[15].

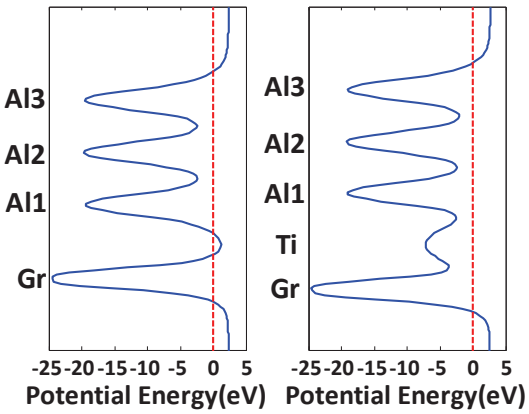

Fig. 3 Potential profiles of Gr/Al and Gr/Ti/Al complexes. Fermi level is set at E=0.

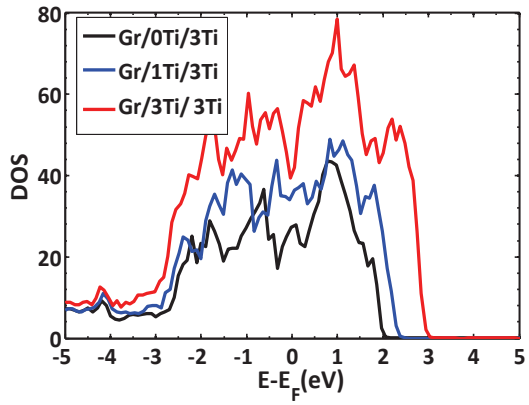

Fig. 4 Potential profiles of Gr/Al and Gr/Ti/Al complexes. Fermi level is set at E=0.

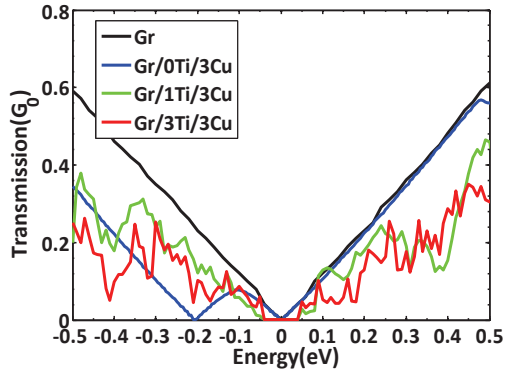

Fig.5 The transmission functions of pure graphene and Gr/Ti/Cu systems at V_{bias}= 0 V. The results of pure Gr and Cu/graphene system are in consistent with Ref. [14]. The conductance dip of Gr/0Ti/3Cu system at -0.2V originates from the Cu-induced Fermi level shift of graphene (ΔE_F).